

Radio-frequency magnetic response of vortex lattices undergoing structural transformations in superconducting borocarbide crystals

R. Prozorov,* V. G. Kogan, M. D. Vannette, S. L. Bud'ko, and P. C. Canfield

Ames Laboratory and Department of Physics and Astronomy, Iowa State University, Ames, Iowa 50011, USA

(Received 8 May 2007; published 26 September 2007)

We report a clear anomaly in the rf response of tunnel-diode resonator measured in rare earth nickel borocarbide crystals with dc applied magnetic field along the crystallographic c axis. We associate the anomaly in the dynamic magnetic susceptibility χ with a structural transition in the vortex lattice. χ is sensitive to the Campbell penetration depth λ_C of the rf perturbation into the mixed state. λ_C depends on the vortex lattice elastic moduli, which in turn depend on the vortex lattice structure. Using this technique, we map the high-field transition line for the square-to-rhombic transformation of the vortex lattice and provide a qualitative argument in favor of thermal vortex fluctuations as a major cause driving the transition.

DOI: 10.1103/PhysRevB.76.094520

PACS number(s): 74.25.Nf, 74.25.Qt, 74.25.Sv, 74.70.Dd

I. INTRODUCTION

In the common picture of type-II superconductors, vortices should form a hexagonal lattice in isotropic or cubic materials; the same should happen in tetragonal materials for applied magnetic fields along the crystallographic c axis. It has been known for a long time that experimentally this is rarely the case.^{1,2} The reason for such behavior was, to a large extent, clarified after nonlocal effects were incorporated into the London description of intervortex interaction.^{3–5} This effort resulted in the realization that the vortex lattice (VL) structure depends on the Fermi surface, the order parameter symmetry, as well as on the applied field, temperature, scattering strength, and even on thermal fluctuations of vortex positions.⁶ Currently, vortex lattice structural phase transitions are best studied in the rare earth nickel borocarbides ($\text{RNi}_2\text{B}_2\text{C} \equiv \text{R1221}$),^{7–15} but, in fact, are present in many superconductors, including cubic Nb and V_3Si .^{16–18}

Information on VL structures is consequential since the VL elastic properties are structure dependent, whereas the vortex dynamics is affected by the lattice elastic moduli.¹⁹ It is worth noting that VL's can be considered as two-dimensional crystals with the densities and interactions easily manipulated by varying the applied field and temperature. The structural transitions discussed here occur because of the competing symmetries of the isotropic London intervortex forces versus the crystal anisotropies, a situation reminiscent of two-dimensional arrangements of adatoms on anisotropic substrates.²⁰

Vortex lattices in R1221 have been probed by Bitter decoration,¹³ small angle neutron scattering (SANS),^{7–10,12} scanning tunneling microscopy (STM),^{11,14} and by muon spin relaxation. Notwithstanding the progress made in locating the transition lines in low fields (an example is given in Fig. 4), the complete mapping of transitions had proven elusive mostly due to reduced sensitivity of these techniques for fields near the upper critical field $H_{c2}(T)$. Calculations based on the Ginzburg-Landau approach¹¹ suggested that the transition line for the transformation of rhombic (triangular) to square (R-S) structures may terminate on the $H_{c2}(T)$ curve. (Hereafter, we are talking about tetragonal crystals in fields

along the c axis.) However, the SANS data on Lu1221 have shown the transition line bending away from $H_{c2}(T)$.¹⁵ Gurevich and Kogan⁶ suggested that softening of the lattice near $H_{c2}(T)$ causes the vortex fluctuations to increase, thus smearing the already weak, square-symmetric contribution to the intervortex interaction and making it isotropic (see also Ref. 21). The model predicts that in small fields, the R-S transition line $H_{\square}(T)$ slowly increases with temperature but then sharply turns upward to avoid $H_{c2}(T)$, becoming a double-valued function.

In this paper, we identify a sharp reversible anomaly seen in the high-frequency response of Y1221 and Lu1221 with the square-to-rhombic transition of the vortex lattice in *high* magnetic fields. We argue, as is done within the weak collective pinning picture, that the ac response of the vortex lattice in high fields is determined not only by classical pinning but also by the thermal disorder, which increases when the upper critical field is approached. This identification is supported qualitatively by estimates of the changes in the lattice elastic moduli which must accompany the square-to-rhombic transition. The anomaly in the dynamic susceptibility is very sharp (as clearly seen in Fig. 1), reversible, and well separated from $H_{c2}(T)$, thus making unlikely that the standard peak effect is the cause of the anomaly existence. Also, the reversible character of the anomaly clearly separates it from the peak effect and from possible depinning transition.

II. EXPERIMENT

The dynamic magnetic susceptibility χ of a superconductor in the mixed state can be measured by the tunnel-diode resonator technique described elsewhere.^{22,23} In short, the frequency shift, Δf , due to a small change in the resonator induction caused by the finite penetration of the ac field into the sample in the mixed state is recorded. This shift is proportional to the change in the dynamic magnetic susceptibility, $\Delta\chi$. In the limit of small amplitude ac excitation fields (0.02 Oe in our case), the nondissipative part $\text{Re}\chi$ is determined by the ac field penetration depth $\delta = (\lambda^2 + \lambda_C^2)^{1/2}$, where λ is the London penetration depth and the Campbell

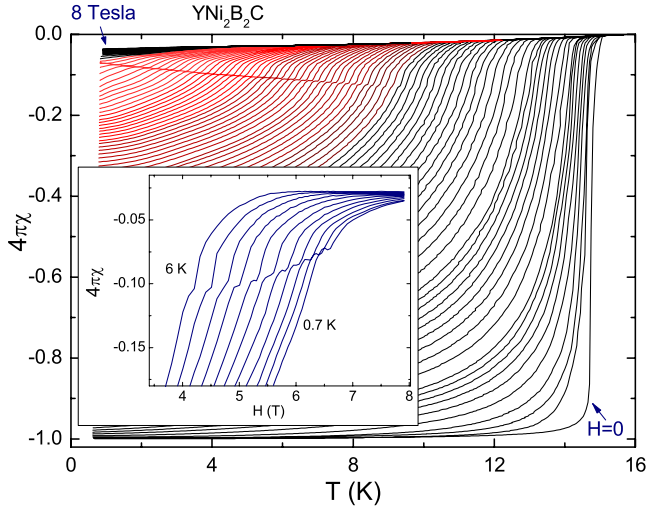


FIG. 1. (Color online) $\chi(T)$ of Y1221 measured in fixed fields with 1 kOe step. The anomaly is clearly seen in the upper left corner. Inset: $\chi(H)$ scans showing the same anomaly.

length λ_C characterizes the pinning and the VL elastic response.^{24,25} For $f \sim 10$ MHz, the skin depth due to the normal excitations vastly exceeds the size of our samples and has no effect on δ . In this work, we utilize the sensitivity of this method to small changes in λ_C that accompany the VL transitions to map the high-field part of the $H_{\square}(T)$ line. Note that the susceptibility we measure is not the same as dM/dH , where M is the dc magnetization, because we are probing the diamagnetic response and the ac perturbation only penetrates to the Campbell depth into a superconductor (analogous to the normal diamagnetic skin effect).

Lu1221 were grown out of Ni_2B flux.^{12,26} Powder x-ray diffraction spectra indicate that there were no detectable second phases present. Y1221 was grown using vertical zone melting method with a commercial four-mirror image furnace (model FZ-T-4000-H-VI-VPM-PC, Crystal Systems Corp., Japan). We have studied both as grown and annealed in active vacuum (950 °C, 48 h) samples³⁰ of a typical size of $1 \times 1 \times 0.1$ mm³. Residual resistance ratios of Lu1221 and Y1221 were about 25, the critical temperatures $T_c \approx 16.2$ and 15.2 K, and $H_{c2}(0) \approx 9.2$ and 8.6 T, respectively. $H_{c2}(T)$ was determined as the onset point of the diamagnetic signal and $H_{c2}(0)$ by extrapolation to $T=0$ (see Fig. 4). Similar values were obtained from resistivity onset as well as by extrapolation technique used in Ref. 26.

III. RESULTS

Temperature scans of the dynamic susceptibility $\text{Re } \chi$ at fixed dc fields from 0 to 8 T for the Y1221 single crystal with $H_{dc} \parallel H_{ac}$ along the c axis are shown in Fig. 1. Hereafter, we deal only with $\text{Re } \chi$ and omit “Re” for brevity; this quantity is normalized so as to have $-1/4\pi$ in the limit $H_{dc} \rightarrow 0$ and to correspond to the full expulsion of the ac signal. There are clear anomalies in the high-field scans, the locus of which appears as a sharp line. The inset of Fig. 1 shows magnetic field scans at constant T with a clearly visible

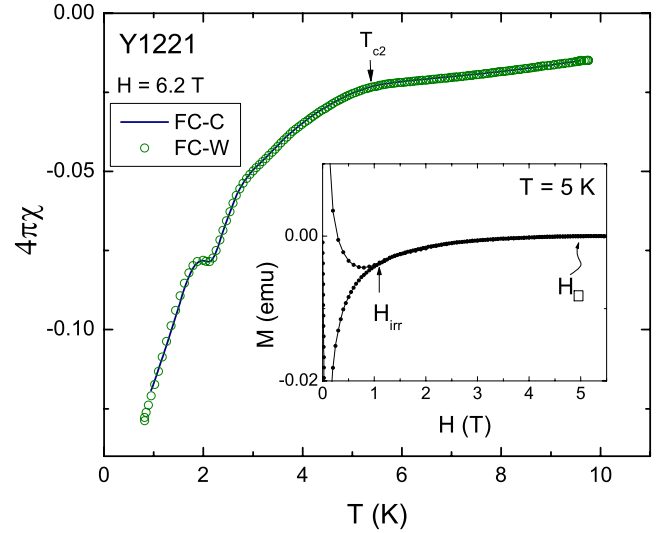


FIG. 2. (Color online) $\chi(T)$ of Y1221 measured in 6.2 T. Open symbols, FC-W; solid line, FC-C as described in the text. Inset: The dc magnetization $M(H)$ measured at 5 K. Indicated are the irreversibility field, H_{irr} , and approximate location of the anomaly, H_{\square} .

anomaly. The positions (H, T) of the anomaly in field sweeps coincide with those observed in $\chi(T)$ scans. Note that the observed anomaly clearly differs from the upper critical field and situated at a sizable distances in T and H from H_{c2} .

We stress that the dc magnetization, $M(H)$, is *reversible* above, under, and within the anomaly, thus excluding irreversibility as possible cause of the observed behavior. This is clearly seen in the inset of Fig. 2. The irreversibility field H_{irr} for the sample of $\text{YNi}_2\text{B}_2\text{C}$ is far from the anomaly; the same is true for all samples used. The main panel of the figure shows an example of $\chi(T)$ at $H=6.2$ T. The sample has been cooled in a fixed field (FC), and after that the temperature has been scanned up (FC-W, open symbols) and down (FC-C, solid line) with no measurable difference in recorded $\chi(T)$. The anomaly, therefore, is unlikely to be caused either by Bragg glass to vortex liquid transition (as discussed in Refs. 27 and 28) or by the differences in pinning reported in Ref. 29.

Figure 3 shows $\chi(T)$ for Y1221 (upper panel) and Lu1221 (lower panel) with a focus on low temperatures and high fields where the anomaly is clearly seen in both samples. Hence, the observed behavior is not limited to a particular sample, but is seen on both mirror-furnace-grown Y1221 and flux-grown Lu1221.

Figure 4 is a summary of the data. As shown in the inset, the curves $H_{c2}/H_{c2}(0)$ vs T/T_c are nearly the same for the two crystals, although the absolute values of H_{c2} 's are somewhat different. For comparison, we show positions of an anomaly in the dc magnetization $M(T)$ of Ref. 31 and the low-field branch of the R-S transition from the SANS data of Ref. 15 (shown with the uncertainty corresponding to various criteria for the peak splitting that mark the R-S transition). The anomaly amplitude decreases with decreasing applied field and increasing temperature (Fig. 3) and the data cannot be extended to the point where they are anticipated to merge with the low-field and high temperature SANS results.

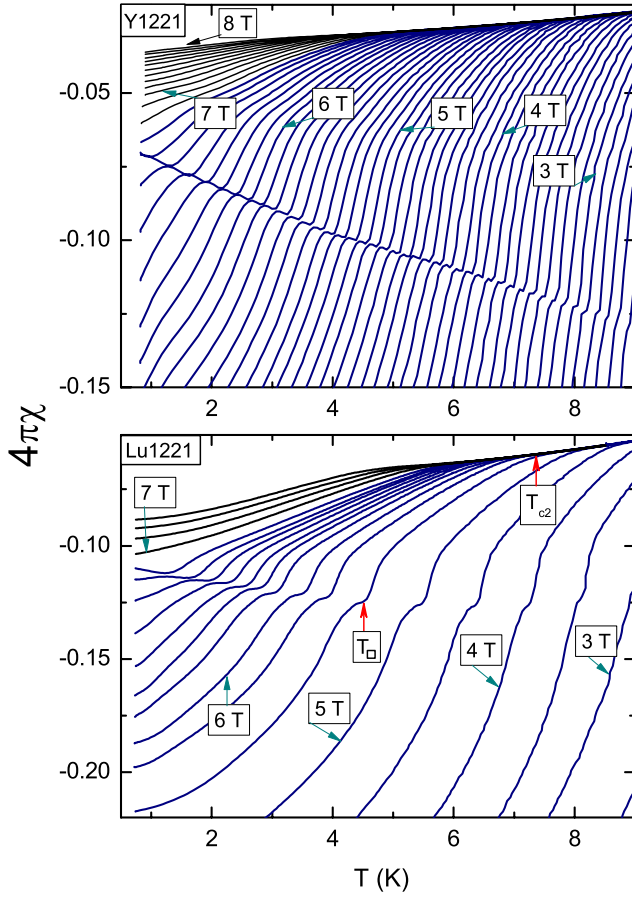


FIG. 3. (Color online) Selected regions of $\chi(T, H)$ curves showing VL transition in Y1221 (top panel) and Lu1221 (bottom panel). At each field, the characteristic temperatures corresponding to $H_{c2}(T)$ line as well as $H_{\square}(T)$ are indicated by arrows at the lower frame.

IV. DISCUSSION

The VL response to a small amplitude ac perturbation is determined by the length^{24,25} given by

$$\delta^2 = \lambda^2 + \frac{H^2}{4\pi K} = \lambda^2 + \frac{cHr_p}{4\pi j_c}, \quad (1)$$

where the term containing the Labusch pinning parameter K is the Campbell λ_C^2 (in high fields, we do not distinguish between H and the magnetic induction). In the second formula, λ_C is expressed in terms of the disorder length r_p and the critical current j_c for the model of *weak collective pinning* expected to hold for high quality crystals of this work.²⁴ For weak disorder and small j_c , $\lambda \ll \lambda_C$. Within the theory of collective pinning, thermal disorder is treated on the same footing as the quench disorder and one can use the relation $r_p^2 = \xi^2 + \langle u^2 \rangle$, where coherence length ξ is taken to be the range of the pinning potential and $\langle u^2 \rangle$ is the mean square thermal fluctuation of vortex positions.¹⁹

The VL shear moduli vanish in the limit $H \rightarrow H_{c2}$, the lattice softens, and $\langle u^2 \rangle$ diverges. As argued in Ref. 6, the nonlocal corrections to the isotropic intervortex interaction

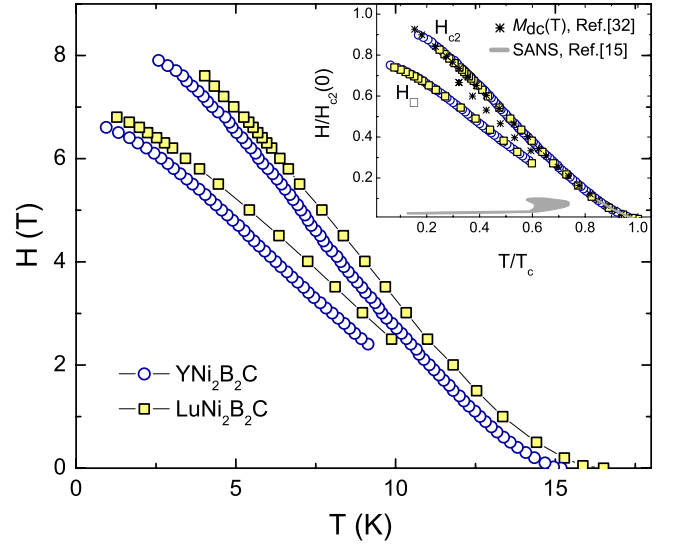


FIG. 4. (Color online) Phase diagram obtained from measurements of $H_{c2}(T)$ and $H_{\square}(T)$. The inset shows the same data in reduced units. Also shown are the results of Ref. 31 and the low-field results of Ref. 15.

responsible for the square structure are washed away, and the lattice near H_{c2} is always triangular (for tetragonal crystals with applied field along the c axis). With decreasing field, the fluctuations weaken, and at some field $H_{\square} < H_{c2}$, the lattice acquires the square structure. The SANS data on cubic V_3Si support this picture.¹⁸ It has been estimated in Ref. 6 that this happens when $\langle u^2 \rangle$ is reduced to values on the order of ξ^2 for clean materials. In most of the domain $H_{\square} < H < H_{c2}$, the fluctuation amplitude exceeds ξ , and for a qualitative discussion we can take $r_p^2 \sim \langle u^2 \rangle$:

$$\delta^2 \approx \frac{cH}{4\pi j_c} \sqrt{\langle u^2 \rangle}. \quad (2)$$

The thermal average $\langle u^2 \rangle$ depends on *all* VL elastic moduli. The number of independent moduli and their values depend on the lattice structure. For fields small on the H_{c2} scale, the moduli were counted and evaluated in Ref. 32 (and in Ref. 21 within the Ginzburg-Landau scheme near T_c). The point relevant for our discussion is that the number of independent moduli depends on the symmetry of the lattice (as within the standard elasticity theory for anisotropic solids³³). When the VL rhombic unit cell with diagonals along $[100]$ and $[010]$ of tetragonal borocarbides (see Refs. 4, 9–11, 14, and 15) transforms to a square, it acquires an extra symmetry associated with the fourfold rotational axis. This reduces the number of independent shear moduli because the shears polarized along $[100]$ and $[010]$ (which are different in the rhombic lattice) become identical. In addition, the squash-shear modulus for the deformation responsible for the transition turns zero at the transition point.^{21,32} One therefore expects $\langle u^2 \rangle$ to be different in the transition vicinity on the two sides of the transition point.

The calculation of this difference at the transition in high fields requires evaluation of the elastic moduli in the pres-

ence of thermal fluctuations, a nontrivial problem to be addressed elsewhere. Still, we can state that with increasing scattering, the domain of the square lattice should shrink and the R-S phase boundary should move to lower reduced fields H_{\square}/H_{c2} .⁶ Physically, this is because the transition to the square structure is caused by the tetragonal symmetry of the Fermi surface and of the order parameter which enter the intervortex interaction through nonlocal corrections to the London theory.³ In low fields, the corrections add the square-symmetric interaction at distances on the order of the nonlocality range ρ which for clean superconductors is on the order of ξ_0 , the zero temperature coherence length. This range, however, shrinks when the mean free path becomes shorter. Hence, one has to go to higher fields for the square-symmetric interaction to cause the R-S transformation. In the high-field domain with fluctuations induced lattice disorder, one has to go to *lower* fields with weaker fluctuations to reach the domain with sufficiently strong nonlocal effects to cause the R-S transition. This happens when $\rho \sim \langle u^2 \rangle$. Since ρ is reduced by scattering, the transition takes place at smaller $\langle u^2 \rangle$, i.e., at lower fields.

To estimate the dynamic susceptibility, we note that in our data $-4\pi\chi \sim 0.1$ at the location of the transition. This implies that, in our case, δ is comparable to or larger than the sample size. A weak screening of the ac field in a disk-shaped sample of a radius R is described by the London-like equation (see, e.g., Ref. 25) $\mathbf{A} - \delta^2 \nabla^2 \mathbf{A} = 0$ for the vector potential $\mathbf{A} = \mathbf{h} \times \mathbf{r}/2 + \mathbf{a}$, where \mathbf{a} is a small correction to the uniform field. This gives

$$\mathbf{h} \times \mathbf{r}/2 \approx \lambda^2 \nabla^2 \mathbf{a} = -4\pi\delta^2 \mathbf{j}/c. \quad (3)$$

Given the current \mathbf{j} , one readily obtains the magnetic moment and $\chi = -R^2/32\pi\delta^2$. Hence,

$$-4\pi\chi = \frac{R^2}{8\delta^2} = \frac{\pi R^2 j_c}{2cH} \langle u^2 \rangle^{-1/2}. \quad (4)$$

If $\langle u^2 \rangle$ varies by $\Delta\langle u^2 \rangle$, the change in the measured quantity is

$$\Delta(-4\pi\chi) = -\frac{\pi R^2 j_c}{4cH \langle u^2 \rangle^{1/2}} \frac{\Delta\langle u^2 \rangle}{\langle u^2 \rangle}. \quad (5)$$

Since $j_c/\langle u^2 \rangle^{1/2}$ decreases on warming, one expects the anomaly size to decrease with increasing T seen in our data. The relative change in the susceptibility is

$$\frac{\Delta\chi}{\chi} = -\frac{\Delta\langle u^2 \rangle}{2\langle u^2 \rangle}. \quad (6)$$

At the transition, $\langle u^2 \rangle \sim \xi_0^2$ for clean materials. As is seen in Fig. 5, $\Delta\chi/\chi \sim 10^{-2}$ in large fields. Hence, our method is sensitive to small changes in thermal averages: $\sqrt{\Delta\langle u^2 \rangle} \sim \xi_0/10$.

It should be noted that, in general, the susceptibility change $\Delta\chi/\chi$ may contain a term $\propto \Delta j_c/j_c$, because the critical current on two sides of the transition may also depend on the vortex lattice elastic properties. Yet, we do not see any measurable difference in the $M(H)$ data and therefore in j_c . It might happen, however, that the nearly static measurement

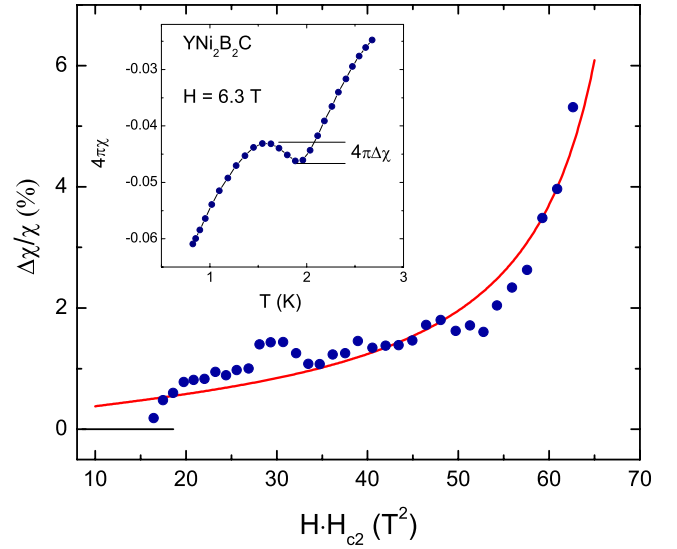


FIG. 5. (Color online) Relative change of χ at the anomaly in Y1221 as a function of $HH_{c2}(T)$. The solid line is a fit to Eq. (9). Inset: The definition of the anomaly size, $4\pi\Delta\chi$.

of $M(H)$ is less sensitive to changes in j_c on a 1% level than the high-frequency response. If so, it would imply that our qualitative model emphasizing the role of fluctuations is oversimplified. Still, the main conclusion that the observed anomaly is related to the structural vortex lattice transition would not alter. We are not aware of any other reason for a sharp change of either j_c or fluctuations at a considerable distance from H_{c2} (e.g., the anomaly width ~ 0.1 T in field of 6.5 T at 0.7 K when $H_{c2} \approx 8$ T). The common peak effect is usually seen in a broad field domain touching H_{c2} and is well pronounced and irreversible in $M(H)$.

The elastic properties of the incompressible square lattice in fixed fields are characterized by four independent moduli which can be chosen as the shear c_x along one of the square diagonals $x \equiv [100]$, the squash c_s transforming the square to a rhombus, the rotation c_r , and the tilt c_{44} . At the transition, $c_s = 0$, whereas according to Ref. 6,

$$\frac{c_r}{c_x} \approx \frac{32\pi\rho^2 \sqrt{HH_{c2}}}{\phi_0} \sim \frac{\sqrt{HH_{c2}(T)}}{H_{c2}(0)} \quad (7)$$

(ρ varies from $0.67\xi_0$ to $0.3\xi_0$ on warming from 0 to T_c in the clean limit). In this situation, Ref. 6 gives $\langle u^2 \rangle \approx f(H, T) \ln(c_x/c_r)$, where f does not depend on the elastic moduli. As is shown in Refs. 6 and 21, only the shear moduli c_{66} change sharply at the transition, so that we estimate

$$\frac{\Delta\langle u^2 \rangle}{\langle u^2 \rangle} \sim \frac{\Delta c_{66}}{c_{66} \ln(c_{66}/c_r)}. \quad (8)$$

The ratio $\Delta c_{66}/c_{66}$ should not depend strongly either on H or on T since the change of the shear moduli is of a geometric nature (due to the symmetry change). We thus expect the following behavior of the measured quantity:

$$-\frac{\Delta\chi}{\chi} \approx \frac{C}{\ln[H_{c2}^2(0)/HH_{c2}(T)]}, \quad (9)$$

with $C \approx \text{const}$. Figure 5 shows the data $\Delta\chi/\chi$ plotted against $HH_{c2}(T)$; the solid line is calculated taking $H_{c2}(0)=8.6$ T with the fit parameter $C=0.76$. The qualitative nature of our argument notwithstanding, we consider this result as supporting our interpretation of the χ anomaly as caused by the R-S structural transformation of the vortex lattice. We note that the anomaly we see for Lu1221 (Fig. 2) does not suffice to extract the jump of χ . This could be due to disorder, the subject of future research.

In Ref. 31, an unusual behavior of the reversible magnetization $M_{dc}(T)$ was interpreted as caused by the R-S transition. As shown in Fig. 4, the position of the anomaly on the H - T phase diagram reported here differs from that of Ref. 31. We did not find an anomaly in $M_{dc}(T, H)$ in our samples.

V. CONCLUSION

In conclusion, we interpret the anomaly in measured $\chi(T, H)$ as caused by the structural transformation of the vor-

tex lattice. We argue that the tunnel-diode resonator has enough sensitivity to measure small changes in the rf penetration depth in the high-field mixed state (i.e., of the Campbell length) which accompany the VL structural transformations. Using this technique, the high-field branch of the rhombic-square lattice transition caused by thermal fluctuations of vortices is determined. We are of course aware of the fact that our measurements do not provide the structural information *per se*, and our conclusions should be verified by direct techniques such as SANS or STM.

ACKNOWLEDGMENTS

We thank J. Yan and G. Lapertot who grew Y1221 crystals in the optical furnace. Work at Ames Laboratory was supported by the Department of Energy, Basic Energy Sciences under Contract No. DE-AC02-07CH11358. R.P. acknowledges support from NSF Grant No. DMR-05-53285 and the Alfred P. Sloan Foundation.

*prozorov@ameslab.gov

¹J. Schelten, in *Anisotropy Effects in Superconductors*, edited by H. Weber (Plenum, New York, 1977), p. 113; B. Obst, *ibid.*, p. 139.

²D. K. Christen, H. R. Kerchner, S. T. Sekula, and P. Thorel, Phys. Rev. B **21**, 102 (1980).

³V. G. Kogan, P. Miranovic, L. Dobrosavljevic-Grujic, W. E. Pickett, and D. K. Christen, Phys. Rev. Lett. **79**, 741 (1997).

⁴V. G. Kogan, M. Bullock, B. Harmon, P. Miranovic, L. Dobrosavljevic-Grujic, P. L. Gammel, and D. J. Bishop, Phys. Rev. B **55**, R8693 (1997).

⁵I. Affleck, M. Franz, and M. H. Sharifzadeh Amin, Phys. Rev. B **55**, R704 (1997).

⁶A. Gurevich and V. G. Kogan, Phys. Rev. Lett. **87**, 177009 (2001).

⁷U. Yaron, P. L. Gammel, A. P. Ramirez, D. A. Huse, D. J. Bishop, A. I. Goldman, C. Stassis, P. C. Canfield, and K. Mortensen, Nature (London) **382**, 236 (1996).

⁸M. R. Eskildsen, P. L. Gammel, B. P. Barber, U. Yaron, A. P. Ramirez, D. A. Huse, D. J. Bishop, C. Bolle, C. M. Lieber, S. Oxx, S. Sridhar, N. H. Andersen, K. Mortensen, and P. C. Canfield, Phys. Rev. Lett. **78**, 1968 (1997).

⁹M. Yethiraj, D. M. Paul, C. V. Tomy, and E. M. Forgan, Phys. Rev. Lett. **78**, 4849 (1997).

¹⁰D. M. Paul, C. V. Tomy, C. M. Aegerter, R. Cubitt, S. H. Lloyd, E. M. Forgan, S. L. Lee, and M. Yethiraj, Phys. Rev. Lett. **80**, 1517 (1998).

¹¹Y. De Wilde, M. Iavarone, U. Welp, V. Metlushko, A. E. Koshelev, I. Aranson, G. W. Crabtree, and P. C. Canfield, Phys. Rev. Lett. **78**, 4273 (1997).

¹²P. L. Gammel, D. J. Bishop, M. R. Eskildsen, K. Mortensen, N. H. Andersen, I. R. Fisher, K. O. Cheon, P. C. Canfield, and V. G. Kogan, Phys. Rev. Lett. **82**, 4082 (1999).

¹³L. Ya. Vinnikov, T. L. Barkov, P. C. Canfield, S. L. Bud'ko, and

V. G. Kogan, Phys. Rev. B **64**, 024504 (2001).

¹⁴H. Sakata, M. Oosawa, K. Matsuba, N. Nishida, H. Takeya, and K. Hirata, Phys. Rev. Lett. **84**, 1583 (2000).

¹⁵M. R. Eskildsen, A. B. Abrahamsen, V. G. Kogan, P. L. Gammel, K. Mortensen, N. H. Andersen, and P. C. Canfield, Phys. Rev. Lett. **86**, 5148 (2001).

¹⁶M. Laver, E. M. Forgan, S. P. Brown, D. Charalambous, D. Fort, C. Howell, S. Ramos, R. J. Lycett, D. K. Christen, J. Kohlbrenner, C. D. Dewhurst, and R. Cubitt, Phys. Rev. Lett. **96**, 167002 (2006).

¹⁷C. E. Sosolik, J. A. Strosio, M. D. Stiles, E. W. Hudson, S. R. Blankenship, A. P. Fein, and R. J. Celotta, Phys. Rev. B **68**, 140503(R) (2003).

¹⁸M. Yethiraj, D. K. Christen, A. A. Gapud, D. M. Paul, S. J. Crowe, C. D. Dewhurst, R. Cubitt, L. Porcar, and A. Gurevich, Phys. Rev. B **72**, 060504(R) (2005).

¹⁹G. Blatter, M. V. Feigel'man, V. B. Geshkenbein, A. I. Larkin, and V. M. Vinokur, Rev. Mod. Phys. **66**, 1125 (1994).

²⁰I. Lyuksyutov, A. G. Naumovets, and V. Pokrovsky, *Two-Dimensional Crystals* (Academic, Boston, 1992).

²¹A. D. Klironomos and A. T. Dorsey, Phys. Rev. Lett. **91**, 097002 (2003).

²²R. Prozorov, R. W. Giannetta, A. Carrington, and F. M. Araujo-Moreira, Phys. Rev. B **62**, 115 (2000).

²³R. Prozorov, R. W. Giannetta, A. Carrington, P. Fournier, R. L. Greene, P. Guptasarma, D. G. Hinks, and A. R. Banks, Appl. Phys. Lett. **77**, 4202 (2000).

²⁴A. E. Koshelev and V. M. Vinokur, Physica C **173**, 465 (1991).

²⁵E. H. Brandt, Phys. Rev. Lett. **67**, 2219 (1991).

²⁶K. O. Cheon, I. R. Fisher, V. G. Kogan, P. C. Canfield, P. Miranovic, and P. L. Gammel, Phys. Rev. B **58**, 6463 (1998).

²⁷S. R. Park, S. M. Choi, D. C. Dender, J. W. Lynn, and X. S. Ling, Phys. Rev. Lett. **91**, 167003 (2003).

²⁸I. K. Dimitrov, N. D. Daniilidis, C. Elbaum, J. W. Lynn, and X. S.

- Ling, Phys. Rev. Lett. **99**, 047001 (2007).
- ²⁹A. V. Silhanek, J. R. Thompson, L. Civale, D. M. Paul, and C. V. Tomy, Phys. Rev. B **64**, 012512 (2001).
- ³⁰X. Y. Miao, S. L. Bud'ko, and P. C. Canfield, J. Alloys Compd. **338**, 13 (2002).
- ³¹T. Park, A. T. Malinowski, M. F. Hundley, J. D. Thompson, Y. Sun, M. B. Salamon, E. M. Choi, H. J. Kim, S.-I. Lee, P. C. Canfield, and V. G. Kogan, Phys. Rev. B **71**, 054511 (2005).
- ³²P. Miranovic and V. G. Kogan, Phys. Rev. Lett. **87**, 137002 (2001).
- ³³L. D. Landau and E. M. Lifshitz, *Theory of Elasticity* (Pergamon, Oxford, 1986).